Determination of the Effective Thermal Conductivity of Aerogel-based Coating Mortars Using Numerical Simulations- Random Packing

Chapter 81
Determination of the Effective Thermal Conductivity of Aerogel-Based Coating Mortars Using Numerical Simulations—Random Packing

Ali Naman Karim and Carl-Eric Hagentoft

Abstract Aerogel-based coating mortars have declared thermal conductivities of 0.03–0.05 W/(m · K), similar to those of conventional thermal insulation materials. Due to the high porosity and fragility of aerogel granules, the material obtains a reduced mechanical strength compared to conventional mortars. Recently, there has been a large research effort on developing new mixtures with improved thermal and mechanical properties. This paper presents and evaluates two-dimensional numerical simulations, based on the random packing technique, as an alternative method to laboratory measurements in predicting the effective thermal conductivity of these mortars. Experimental data from the literature, on thermal conductivity of aerogel-based coating mortars containing 50–90 vol% aerogels were used to validate the simulation results. In this preliminary validation study, a relative error of 6–10% was observed. Future work can focus on improving the accuracy and including the prediction of mechanical properties in the suggested model.

Keywords Aerogel · Coating mortar · Effective thermal conductivity · Random packing technique · Numerical simulations

81.1 Introduction

Aerogel-based Coating Mortars (ACM) are a class of multifunctional wall finishes, plasters and renders, that are recognized for their improved thermal insulation properties (Karim et al. 2022). ACMs incorporate high fraction (more than 50 vol%) of aerogel granules. Aerogel is a superinsulation material with high porosity, low density, low mechanical strength, and low thermal conductivity. The thermal conductivity of aerogels is within 0.010–0.020 W/(m · K), i.e., lower than of stagnant air (0.026 W/(m · K)). Due to the addition of aerogel granules in ACMs, commercial products have a declared thermal conductivity of about 0.03–0.05 W/(m · K) that

A. N. Karim (✉) · C.-E. Hagentoft
Department of Architecture and Civil Engineering, Chalmers University of Technology, Gothenburg, Sweden
e-mail: ali.karim@charlmers.se

L. L. Wang et al. (eds.), *Proceedings of the 5th International Conference on Building Energy and Environment*, Environmental Science and Engineering,
https://doi.org/10.1007/978-981-19-9822-5_81

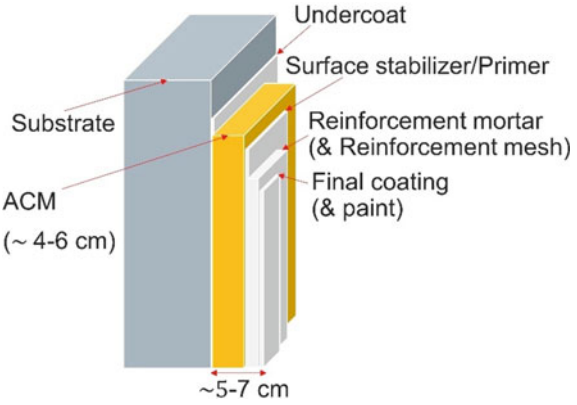

Fig. 81.1 Schematic, illustrating a multilayer coating system including ACM (Karim et al. 2022)

is comparable to the same for conventional thermal insulation materials. Similar to conventional coating mortars, AMCs can be applied manually by hand or by using spray machines.

ACMs are considered as promising alternatives for improving the thermal performance of wall elements, especially when retrofitting old and historical buildings. By using ACMs on façades, the energy efficiency can be improved as well as slimmer wall elements can be achieved. On the other hand, the ACMs suffer from reduced mechanical strength compared to conventional coating mortars. As such, ACMs are in practice applied on surfaces as part of a multilayer coating system (Fig. 81.1) to protect the ACM from mechanical and climatic stresses.

Recently, a lot of research effort has been made on evaluating and improving the mechanical strength of the material without compensating its thermal performance (Ximenes et al. 2016; de Fátima Júlio et al. 2016; Westgate et al. 2018). Most of these studies are based on several time-consuming laboratory-based measurements where the material composition of the samples is modified. Such optimization studies, require large number of samples to be casted, cured and dried out before the actual measurements can be conducted. As an attempt to contribute to this research topic, this paper studies the feasibility of numerical simulations, using random packing technique, to predict the Effective Thermal Conductivity (ETC) of ACMs with various material compositions. The intention is to suggest a time-efficient alternative method with sufficient accuracy, to reduce the number of required laboratory measurements when optimizing the material properties of new ACMs. The suggested method has been used previously for other building materials with accepted accuracy (Chen et al. 2015; Mirzanamadi et al. 2018). However, to the authors' best knowledge, the method has not been tested and validated for materials such as ACMs with high proportion of aerogel granules, and high porosity.

81.2 Methods

In this paper, two-dimensional (2D) numerical thermal simulations were used to predict the ETC of ACMs with various proportion of aerogel. At first a three-phase microstructure model, representing the binder, aggregates (aerogel granules) and air voids, was generated using the random packing technique. Second, the ETC of the generated sample was calculated at steady state using the finite element method. Finally, a set of experimental data from literature was used to validate the calculated results. In this section, the calculation steps are presented in detail.

81.2.1 Microstructure Generation: Random Packing

The microstructure of the ACMs was generated in MATLAB (R2017b) based on a hierarchically based multiscale approach, adapted from Chen et al. (2015), Mirzanamadi et al. (2018). In this method, components for the dispersed phases (aerogels and air voids) were randomly generated and placed in the matrix for the third phase (binder). At first, a square box (50 mm × 50 mm), with a size 12.5 times larger than the largest component size in the studies (4 mm), was generated representing the binder. The amount of each phase (aerogel and air) was later calculated for the generated square box, based on their volume fraction in the mixture. Both the aerogel granules and air voids were assumed to have circular cross-sections of same size (diameter), to simplify and speed-up the generation process. In (Mirzanamadi et al. 2018), Mirzanamadi et al. stated that the impact of the selected shape and size of the components in the generated microstructures was less significant (less than 1%) for the result. In this paper, all air voids were given a diameter of 1 mm, adapted from Mirzanamadi et al. (2018). For simplicity, the diameter of aerogels was set to 4 mm. This simplification was based on the fact that the aerogels, used in the exprimental measurements extracted from litterature, had diameters of 1.2–4 mm.

Next, the components for each phase were placed randomly and one by one in the square box. Once a component was placed, the position was no longer available for the next component. The adapted generation method implied also that no overlapping was allowed. If any overlapping, the component was given a new random position instead. This process continued until all the components were positioned in the box. In (Mirzanamadi et al. 2018), the component for all phases were generated at once and in one numerical sample. In (Chen et al. 2015), Chen et al. employed several metrices instead to generate the final multistructures. The reason was that it was impossible to fit all components simultaniously in the box. In this paper, the first method chosen in Mirzanamadi et al. (2018) was considered at first. In Fig. 81.2, an example of a generated microstructure is shown.

However, the generation script failed to generate microstructures with higher proportion of aerogels and air voids (above 70%). Thus, the second multistep approch suggested in Chen et al. (2015) was selected. As illustrated in Fig. 81.3, the air voids

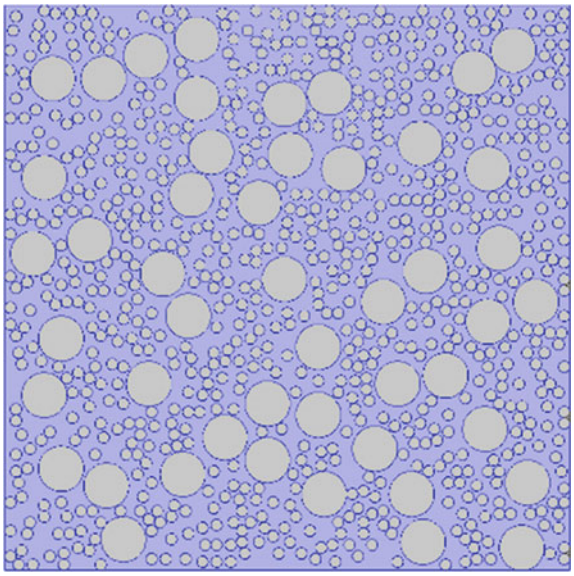

Fig. 81.2 Generated microstructure of a numerical sample consisting of 25% aerogel (larger circles) and 26% air voids (smaller circles) when packing all components in one step

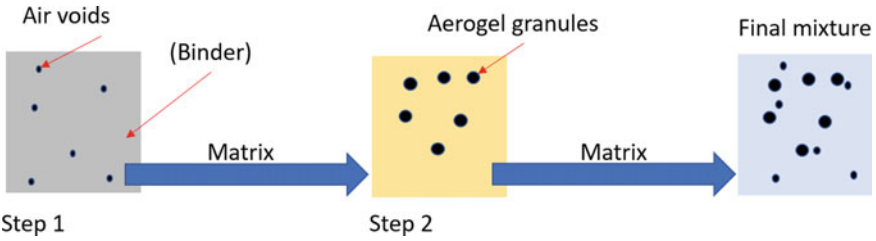

Fig. 81.3 Schematic illustrating the process of packing the components and generating the numerical samples in this study

were first generated and positioned in the box of the binder. Next, the generated microstructure was considered as the matrix of the new and final microstructure where the aerogel granules were added. For each mixture of ACMs studied in this paper, three sets of randomly-packed numerical samples were generated and examined.

81.2.2 Numerical Simulations

Once a microstructure was generated in MATLAB, it was imported to COMSOL (5.4) using the MATLAB-COMSOL interface LiveLink. In COMSOL, the finite element

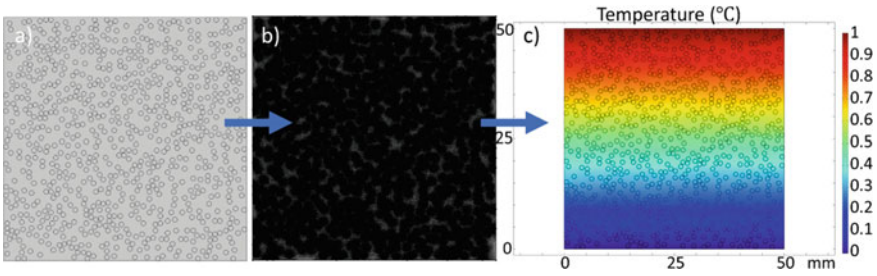

Fig. 81.4 Calculation process of the ETC of a numerical sample. **a** importing the generated geometry to COMSOL. **b** meshing of the domain. **c** Solving of the heat transfer equation

analysis considering the one-dimensional heat transfer was conducted and the ETC of the numerical samples was calculated. In Fig. 81.4, the process of calculating the ETC of a numerical sample in COMSOL is illustrated. For meshing of the domain, the free meshing technique using triangular elements (size: "extremely fine") in COMSOL was selected. The ETC of each sample was calculated at steady state at two principal directions. For this purpose, a heat flux was generated inside the sample by applying a temperature difference of one degree over the cross-sections (top to bottom and right to left). The other two surfaces were set to adiabatic, using the heat insulation condition in COMSOL. The final ETC of each mixture was calculated as the mean value of all three samples and in both directions. The total time to conduct the calculation process for all three sets of each numerical sample was less than an hour.

In the default analyses, the only heat transfer mechanism considered was conduction while long-wave radiation and convection were neglected. In the second round of the analyses, a simplified approach was adapted to consider the radiative heat transfer inside the samples and through the pore walls. As such, an equivalent radiative thermal conductivity, λ_{rad} (W/(m · K)), at the pore scale was introduced, see Eq. (81.1) (Mirzanamadi et al. 2018).

$$\lambda_{rad} = 4 \cdot \varepsilon \cdot \sigma \cdot d_{\max} \cdot \gamma \cdot T^3 \tag{81.1}$$

In Eq. (81.1), ε (−) is the emissivity of matrix walls, set to 0.9. σ is the Stephan-Boltzmann constant ($5.76 \cdot 10^{-8}$ W/$\left(\mathrm{m}^2 \cdot \mathrm{K}^4\right)$), d_{max} (m) is the maximum distance between the pores, γ (-) is the geometrical factor set to $\pi/4$ for circular particles, and T (K) is the (mean) temperature of the pore walls. By adding λ_{rad} to the thermal conductivity of the air voids, λ_{air} (W/(m · K)), a new thermal conductivity for the air voids, λ^*_{air} (W/(m · K)), was introduced, see Eq. (81.2). Using the new thermal conductivity for the air voids, the radiative heat transfer was considered as a conductive heat transfer process in the analyses.

$$\lambda^*_{air} = \lambda_{air} + \lambda_{rad} \tag{81.2}$$

Table 81.1 Composition of the constructed samples in the experimental study (Nosrati and Berardi 2018)

Sample	Plaster (vol%)	Aerogel (vol%)	Water (vol%)
Pure plaster	73	0	27
25% aerogel	49	25	26
50% aerogel	30	50	20
70% aerogel	15	70	15
80% aerogel	6	80	14
90% aerogel	3	90	7

81.2.3 Validation: Experimental Measurements

To evaluate the accuracy of the suggested method, experimental data presented in Nosrati and Berardi (2018) were used. In (Nosrati and Berardi 2018), Nosrati and Berardi constructed samples of ACMs by mixing a high performance hydraulic lime-based plaster with various fraction (0–90 vol%) of silica aerogels (P300) and measured their thermal conductivity at dry state (Relative humidity of 0%). In Table 81.1, the material composition of the constructed samples is presented. In this validation study, samples with an aerogel proportion greater than 50% were considered as it is essential to reach down to thermal conductivities of the currently available ACMs (0.03–0.05 W/(m · K)). As the porosity (air content) of the samples in Nosrati and Berardi (2018) was not specified, a simplification was made assuming that the volume fraction of water used in the fresh mortar roughly matched the fraction of air voids in the hardened sample. The thermal conductivity of air and aerogel was set to 0.026 (Hagentoft 2001) and 0.022 W/(m · K) (Cabot Corporation 2022), respectively. The thermal conductivity of plaster, i.e., the solid part of the sample of pure plaster in Table 81.1, was calculated to 0.2 W/(m · K).

81.3 Results

The ETC of numerical samples of ACMs with 50–90 vol% of aerogel granules was calculated using the presented model. In Table 81.2, the calculated results are compared to the measured values in Nosrati and Berardi (2018). The calculated values for each sample, represents the mean value of all three sets of randomly packed microstructures. As seen in Table 81.2, the numerical model always predicted lower ETCs compared to the experimentally measured ones. The relative error presented was calculated by the difference between the calculated and measured values divided by the measured value. The relative error for the default calculations considering conductive heat transfer was between 7 and 11%. In the second attempt, when radiation was considered, the relative error (Error-radiation) was reduced to be between 6 and 10%.

Table 81.2 Comparison between the calculated ETCs W/(m · K) and the measured values W/(m · K) presented in Nosrati and Berardi (2018)

Sample	Experiment	Numerical simulation	Numerical simulation-radiation	Error (%)	Error-radiation (%)
50% aerogel	0.0694	0.0641	0.0655	7.6	5.6
70% aerogel	0.0306	0.0284	0.0290	7.1	5.2
80% aerogel	0.0261	0.0244	0.0249	6.4	4.7
90% aerogel	0.0257	0.0230	0.0232	10.5	9.7

81.4 Discussion

In this paper, numerical simulations were performed to predict the ETC of ACMs with high proportion of aerogel granules. The intention with the proposed method was to present an alternative method to the time-consuming laboratory measurements and to speed up the development and optimization process of new ACMs. A such, the model must be simple and time efficient that does not require a high computational effort. For this reason, a 2D numerical approach was considered in this study instead of 3D, although the latter may have resulted in more accurate predictions. In the study conducted by Chen et al. (2015), the difference between the calculated ETCs in 2D and 3D was around 5% which in some cases may be significant. On the other hand, a 3D simulation will most likely be more time consuming and reuiring a noticablly higher computational effort that may not be in line with the main purpose of the model.

In the suggested model, several assumptions and simplifications were made. When generating the microstructures, the components of each phase (aerogel and air) were assumed to be of circular cross-sections, all having the same size. This was a rough simplification to reduce the complexity of the microstructure and to speed up the process. However, both the size and shape of the components may vary in real samples. Although the shape of the components was considered to be of less importance in Mirzanamadi et al. (2018), the assumption on the size and shape of the components should be evaluated more in future.

The default analyses conducted in this paper, considered only conduction while convection and radiation were neglected. Also, the developed model neglected the latent heat transfer through evaporation as the experimental measurements were stated to have been performed at dry state. As an attempt to consider the heat transfer through radiation, a simplified method was adapted introducing an effective thermal conductivity for the air voids that included radiation. The inclusion of heat transfer through radiation, reduced the relative error by approximately 1%. Here, the simplifications made on the shape and size of the air voids may have an important impact

on the outcome of the analyses. As the calculated values by the model underestimated the ETC of the samples, it is recommended to study further the impact of these assumptions.

In the preliminary validation study conducted in this paper, an assumption was made on the volume fraction of air voids in the samples used in the measurements. As the porosity of the sample was not measured in the literature, the volume fraction of water in the fresh mortar was considered as the volume of air in the hardened product. This assumption is not necessarily a valid one. Part of the water used in fresh mortar will normally be chemically bonded. Also, the final porosity in the sample is dependent on other circumstances during the curing phase such as ambient temperature. However, when developing new mixtures of ACMs with new material compositions, it is rather likely that the porosity in the final mixture is not identified unless performing laboratory measurements. As the purpose of the suggested model is to avoid time consuming laboratory measurements, this assumption may be accepted as a simple solution for the lack of knowledge about the porosity. In the continuation of the work, more validation studies will be required before the validity of these assumptions can be confirmed.

81.5 Conclusions

In this paper, a two-dimensional numerical simulation model based on random packing technique was proposed to predict the effective thermal conductivity of aerogel-based coating mortars. The intention was to propose a more time-efficient alternative method than laboratory measurements for predicting the effective thermal conductivity of new aerogel-based coating mortars with acceptable accuracy. The results of the first validation study showed a relative error of 6–10% between the calculated and measured values. As of the current stage of development, the accuracy of the model can be considered sufficient. In the continuation of the work, it is suggested to focus on increasing the accuracy of the model. In addition, due to the importance of both the mechanical and thermal properties of these mortars, the model can ideally be further developed to be able to predict the mechanical properties as well as the thermal properties.

References

Cabot Corporation (2022) Specialty chemicals and performance, aerogel particles- P300, [Online]. Available: https://www.cabotcorp.com.ar/solutions/products-plus/aerogel/particles

Chen J, Wang H, Li L (2015) Determination of effective thermal conductivity of asphalt concrete with random aggregate microstructure. J Mater Civ Eng 27(12):04015045

de Fátima Júlio M, Ilharco LM, Soares A, Flores-Colen I, de Brito J (2016) Silica-based aerogels as aggregates for cement-based thermal renders. Cem Concr Compos

Hagentoft CE (2001) Introduction to building physics. Student literature

Karim AN, Johansson P, Sasic Kalagasidis A (2022) Knowledge gaps regarding the hygrothermal and long-term performance of aerogel-based coating mortars. Constr Build Mater 314:125602
Mirzanamadi R, Johansson P, Grammatikos SA (2018) Thermal properties of asphalt concrete: a numerical and experimental study. Constr Build Mater 158:774–785
Nosrati RH, Berardi U (2018) Hygrothermal characteristics of aerogel-enhanced insulating materials under different humidity and temperature conditions. Energy Build 158:698–711
Westgate P, Paine K, Ball RJ (2018) Physical and mechanical properties of plasters incorporating aerogel granules and polypropylene monofilament fibres. Constr Build Mater 158:472–480
Ximenes S, Silva A, Soares A, Flores-Colen I, de Brito J (2016) Parametric analysis to study the influence of aerogel-based renders' components on thermal and mechanical performance. Materials (basel) 9(5):336–355